

# Crystalline Nanoporous Materials Based on Poly(2,6-dimethyl-1,4-phenylene)oxide

Christophe Daniel,\*<sup>1</sup> Simona Longo,<sup>1</sup> Michele Galizia<sup>2</sup>

**Summary:** Different types of crystalline nanoporous materials (powders, films, aerogels) based on poly(2,6-dimethyl-1,4-phenylene)oxide can be easily obtained depending on the preparation procedures. The nanoporous nature of the crystalline phase confers to these materials peculiar transport properties which make them particularly interesting for a potential use as a sorption medium to remove traces of pollutants from water and air or for membrane based gas separation processes. Different aspects relative to the structure and the transport properties of these new polymeric materials are described.

**Keywords:** aerogels; nanoporous crystalline phase; poly(2,6-dimethyl-1,4-phenylene) oxide; supercritical carbon dioxide

## Introduction

The existence of polymer-solvent co-crystalline phases, i.e. structures where a polymeric host and a low-molecular-mass guest are co-crystallized, has been reported for many polymers<sup>[1]</sup> like e.g. isotactic<sup>[2]</sup> and syndiotactic polystyrene (s-PS),<sup>[3]</sup> syndiotactic poly-*p*-methyl-styrene,<sup>[4]</sup> syndiotactic poly-*m*-methyl-styrene,<sup>[5]</sup> polyethylene-oxide,<sup>[6]</sup> poly(vinylidene fluoride),<sup>[7]</sup> syndiotactic polymethylmethacrylate,<sup>[8]</sup> isotactic poly-4-methyl-1-pentene<sup>[9]</sup> or poly(2,6-dimethyl-1,4-phenylene ether) (PPO).<sup>[10]</sup>

The removal of the guest molecules from polymer co-crystalline forms generates polymer chain rearrangements, generally leading to crystalline forms that are densely packed and exhibit a density higher than that one of the corresponding amorphous phase. However it has been discovered that in few cases (to our knowledge, up to now only for s-PS and PPO), by using suitable guest removal conditions, nano-

porous crystalline forms (microporous by IUPAC definition) characterized by empty spaces, exhibiting a density lower than that of the corresponding amorphous phases can be obtained.<sup>[11,12,15]</sup>

The existence of nanoporous polymeric crystalline phases has been first described for syndiotactic polystyrene (s-PS).<sup>[11,12]</sup> This commercially available thermoplastic polymer which is able to form co-crystalline phases with several low-molecular-mass guest molecules can also give, in turn, by suitable guest extraction procedures, two nanoporous crystalline forms named  $\delta$  (monoclinic, with empty space organized as cavities<sup>[11]</sup>) and  $\epsilon$  (orthorhombic, with empty space organized as channels<sup>[12]</sup>). Both crystalline frameworks rapidly absorb volatile organic molecules (mainly halogenated or aromatic hydrocarbons), even if present in traces in air or water<sup>[13]</sup> and hence are promising for applications in chemical separations and molecular sensorics.<sup>[14]</sup>

Very recently it has been shown that poly(2,6-dimethyl-1,4-phenylene)oxide (PPO) can also form various nanoporous crystalline phases<sup>[15]</sup> presenting much higher solubility of many guests (e.g., benzene,<sup>[15]</sup> CCl<sub>4</sub>,<sup>[15]</sup> CO<sub>2</sub>,<sup>[16]</sup> methane,<sup>[16]</sup> propane,<sup>[16]</sup> and propene<sup>[16]</sup>) than fully amorphous PPO. Moreover with respect

<sup>1</sup> Dipartimento di Chimica e Biologia, Università degli Studi di Salerno, Via Ponte don Melillo, 84084 Fisciano (SA), Italy  
E-mail: cdaniel@unisa.it

<sup>2</sup> Department of Chemical, Materials and Production Engineering, University of Naples Federico II, p.le Tecchio 80, 80125 Napoli, Italy

to s-PS, PPO presents the advantage to also possess a high melting temperature of the nanoporous crystalline phases at c.a. 250 °C<sup>[17]</sup> while the  $\delta$  and  $\epsilon$  phases of s-PS transform into the dense  $\gamma$  crystalline phase at c.a. 120 °C.<sup>[18]</sup>

In this contribution different aspects relative to the structure and the sorption properties of different materials (powder, film and aerogels) based on nanoporous crystalline PPO will be presented and discussed.

## Experimental Part

PPO was purchased by Sigma Aldrich and presents weight-averaged and number-averaged molecular masses  $\overline{M}_w = 57700$  g/mol and  $\overline{M}_n = 16600$  g/mol s-PS was manufactured by Dow Chemicals under the trademark Questra 101. <sup>13</sup>C nuclear magnetic resonance characterization showed that the content of syndiotactic triads was over 98%. Weight-averaged and number-averaged molecular masses were found to be  $M_w = 320000$  g/mol and  $M_n = 82000$  g/mol. Solvents were purchased from Aldrich and used without any further purification.

PPO and mixed PPO/s-PS gel samples were prepared in hermetically sealed test tubes by heating the mixtures above the boiling point of the solvent until complete dissolution of the polymer and the appearance of a transparent and homogeneous solution had occurred. Then the hot solution was cooled down to room temperature where gelation occurred.

PPO amorphous films were obtained by compression molding after melting at 290 °C of the as-purchased PPO. The crystallization of these amorphous films has been induced by exposure to the vapors of different solvents at room temperature.

Solvent extraction from PPO gels, mixed PPO/s-PS gels, and PPO crystallized films was carried out by treating the samples with a SFX 200 supercritical CO<sub>2</sub> extractor (ISCO Inc.) using the following conditions: T = 40 °C, P = 250 bar, extraction time t = 180 min.

X-ray diffraction patterns were obtained on a Bruker D8 automatic diffractometer operating with a nickel-filtered Cu K $\alpha$  radiation.

The morphology of the aerogel monoliths was characterized by means of a scanning electron microscope (SEM, Zeiss Evo50 equipped with an Oxford energy dispersive X-ray detector).

Surface area, pore volume and pore size distribution were obtained by N<sub>2</sub> adsorption measurements carried out at 77 K on a Micromeritics ASAP 2020 sorption analyzer. All the samples were outgassed for 24 h at 30 °C before the analysis.

The solvent vapour sorption measurements have been carried out at 35 °C with a VTI-SA symmetrical vapour sorption analyzer from TA instruments.

Subatmospheric gas sorption experiments have been carried out using a CAHN D200 electronic microbalance (CAHN Instruments, Madison, WI), with a sensitivity of 0.1  $\mu$ g. Experimental details and the method used to determine the solubility and diffusivity values are given in ref.<sup>[16]</sup>

## Results and Discussion

### Nanoporous PPO Powders

The treatment of PPO gels with supercritical carbon dioxide allows a complete removal of the solvent initially present in the gels and solvent free powder samples are obtained.

Typical x-ray diffraction patterns of PPO powders, as obtained from gels in benzene, CCl<sub>4</sub>, and decalin after complete solvent extraction by supercritical carbon dioxide, are shown in Figure 1a, b, and c.

The X-ray diffraction patterns of the powders from benzene, and CCl<sub>4</sub> gels (Figures 1a and 1b) exhibit high degrees of crystallinity (in the range 50–60%) and present peaks being located at different diffraction angles. Conversely, the diffraction pattern of the powders from decalin gels presents only a broad amorphous halo (Figure 1c) indicating the formation of fully amorphous PPO.

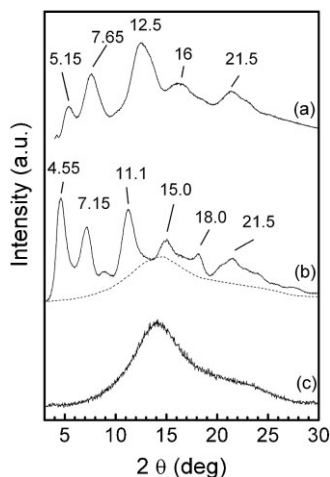


**Figure 1.**

X-ray diffraction patterns (CuK $\alpha$  radiation) of PPO powder samples, after complete solvent extraction by supercritical carbon dioxide, as obtained from gels in benzene (a), CCl<sub>4</sub> (b) and decalin (c); the dashed line corresponds to the amorphous halo used for the determination of the degree of crystallinity for the sample obtained from the PPO/CCl<sub>4</sub> gel.

The diffraction data reported in Figure 1 indicate that, depending on the solvent, different crystalline phases can be obtained after solvent removal from the gels. It is worth adding that additional crystalline

phases have been obtained after treatment with supercritical carbon dioxide of PPO gels prepared in other solvents such as  $\alpha$ -pinene, 1,2-dichloroethane, tetralin,...<sup>[15]</sup>

N<sub>2</sub> isotherms for these semi-crystalline and amorphous PPO powders obtained after supercritical CO<sub>2</sub> treatment of the gels are compared in Figure 2 and the surface area, total pore volume, and micropore volume of the different PPO powder samples are reported in Table 1.

The large surface area and pore volume possessed by the three PPO samples are noteworthy, with an important contribution due to the presence of micropores (namely pores <2 nm according to IUPAC definition). Particularly interesting is the result that the porosity and microporosity of semi-crystalline samples are much higher than the ones of the fully amorphous sample.

The N<sub>2</sub> sorption experiments clearly show that nanoporous (or microporous according to IUPAC definition) crystalline phases are obtained by solvent extraction from PPO gels.

For the case of s-PS it has been observed that the presence of a nanoporous crystalline phases leads to high sorption uptake values of VOC traces from air or water.<sup>[13]</sup>

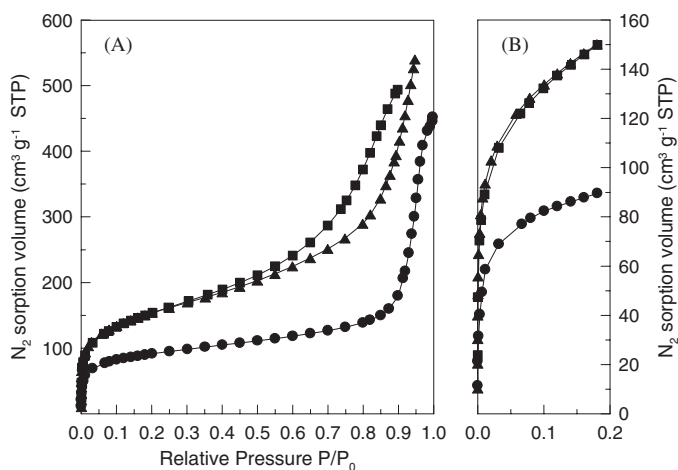


**Figure 2.**

Volumetric N<sub>2</sub> adsorption isotherms recorded at 77 K on PPO samples, after complete solvent extraction by supercritical carbon dioxide, as obtained from gels in decalin (●), benzene (■) and CCl<sub>4</sub> (▲). B shows the detail of the adsorption branch reported in A, for low pressures.

**Table 1.**

Surface area ( $\text{m}^2 \text{g}^{-1}$ ) and pore volume ( $\text{cm}^3 \text{g}^{-1}$ ) of PPO samples which  $\text{N}_2$  adsorption isotherms are reported in Figure 2.

	$S_{\text{BET}}^{\text{a}}$	$S_{\text{micro}}^{\text{a}}$	$V_{\text{tot}}^{\text{b}}$	$V_{\text{micro}}^{\text{c}}$
from PPO/ $\text{CCl}_4$ gel (semi-crystalline sample)	549	214	0.64	0.12
from PPO/benzene gel (semi-crystalline sample)	552	171	0.47	0.10
from PPO/decalin gel (amorphous sample)	320	102	0.28	0.06

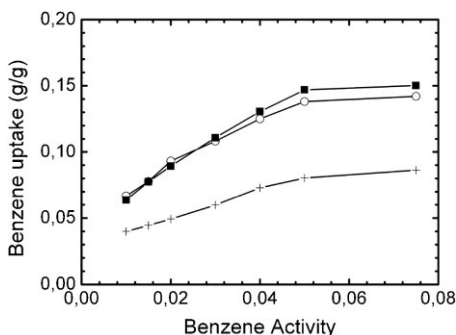
<sup>a</sup> Total area evaluated following the BET model in the standard  $0.05 < P/P_0 < 0.25$  pressure range.

<sup>b</sup> Total pore volume calculated as volume of the liquid at  $p/p_0 \approx 0.90$ .

<sup>c</sup> Micropore volume obtained from the t-plot.

Benzene sorption experiments at  $35^\circ\text{C}$  and pressures lower than  $0.08 P/P_0$  on amorphous powder from a decalin gel (of Figure 1c) and semi-crystalline PPO powders obtained from gels in benzene (of Figure 1a) and in  $\text{CCl}_4$  (of Figure 1b) have been conducted and results are reported in Figure 3.

It is clearly apparent that large solvent uptakes occur for all PPO samples already at very low solvent activities, which is consistent with the presence of nanopores. However, the lowest solvent equilibrium uptake occurs for the amorphous powder while the guest uptake of the two highly crystalline PPO powders is roughly double with respect to those of the amorphous powder. This result is consistent with the  $\text{N}_2$  sorption data which show that semi-crystalline samples possess a microporosity nearly double than the fully amorphous sample (column 5 of Table 1).

**Figure 3.**

Benzene gravimetric sorption isotherms, at  $35^\circ\text{C}$  and at pressures lower than  $0.08 P/P_0$ , on PPO samples: amorphous from a gel with decalin (+); semi-crystalline from a gel with benzene (■) and semi-crystalline from a gel with  $\text{CCl}_4$  (○).

### Nanoporous PPO Aerogels

For syndiotactic polystyrene it has been shown that the sorption kinetics<sup>[19]</sup> but also the uptake values<sup>[20]</sup> for molecules presenting a poor solubility in the polymer amorphous phase depend on the sample morphology. In particular it has been observed that both kinetics and uptake values can be greatly increased by using aerogels instead of powder or film samples. Sorption experiments of 1,2-dichloroethane from diluted aqueous solutions have shown that the use of aerogels with the crystalline nanoporous  $\delta$  – form can result in an apparent increase in the guest diffusivity of several orders of magnitude (up to 7), with respect to  $\delta$ -form films.<sup>[19b]</sup>

However, conversely to s-PS, the solvent extraction from the gels leads, in the case of PPO, to powders or extremely brittle samples rather than to robust aerogels.<sup>[21]</sup> This result can be explained by the different morphologies obtained in s-PS and PPO gels.

The Scanning Electron Microscopy (SEM) images of a s-PS/1,2-dichloroethane and a PPO/1,2-dichloroethane gel prepared at  $C_{\text{pol}} = 20 \text{ wt}\%$  and then treated with supercritical carbon dioxide are shown in Figure 4A and 4B, respectively.

The SEM images clearly show the different morphologies of the s-PS and PPO samples prepared in the same conditions. In fact, the s-PS aerogel (Figure 4A) presents a fibrillar morphology with fibrils diameter of 60–150 nm, while the PPO nanoporous-crystalline powder exhibits globular morphology (Figure 4B), possibly constituted by aggregates of spherulites.

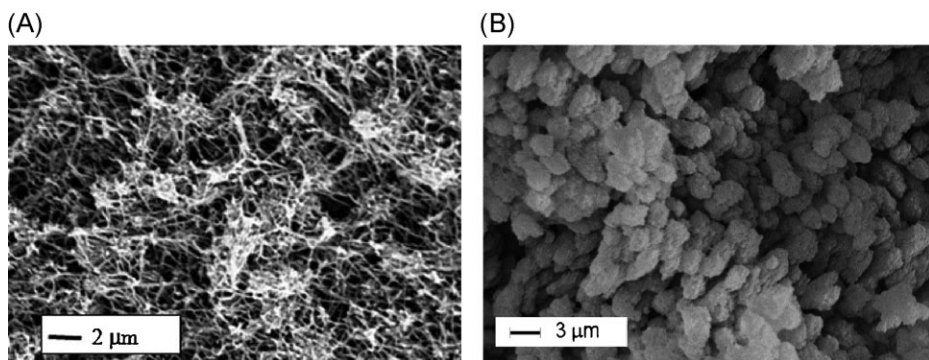


**Figure 4.**

SEM images of samples, as prepared from DCE gels with polymer content of 20wt%, after complete solvent extraction by supercritical CO<sub>2</sub>: (A) s-PS; (B) PPO.

PPO based aerogels can be prepared, however, from mixed PPO/s-PS gels. This is shown, for instance in Figure 5A, for a PPO/s-PS (90/10) gel in 1,2-dichloroethane with a total polymer content of 20 wt%.

During solvent extraction the shape and the dimensions of the mixed s-PS/PPO

gel remain substantially unchanged and the obtained aerogels exhibit a toughness comparable to those of s-PS.

The SEM images of the aerogel obtained from PPO/s-PS blend (Figure 5B) clearly show the maintenance of the fibrils typical of s-PS aerogels, together with a size-

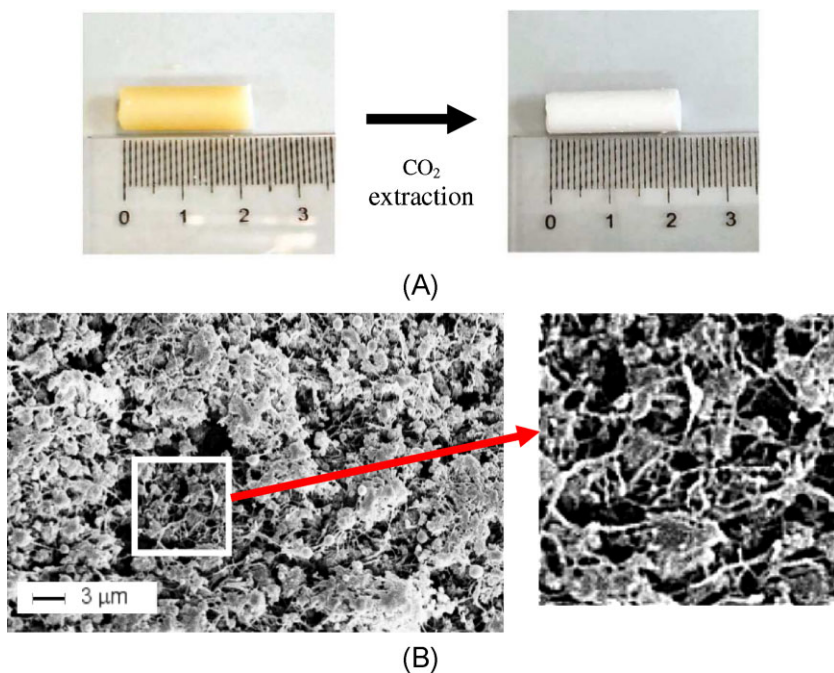


**Figure 5.**

(A) Photographs of pieces of PPO/s-PS, 90/10 wt/wt gels prepared in 1,2-dichloroethane with a polymer concentration of 20 wt%, before and after complete solvent extraction via supercritical carbon dioxide (units in the ruler are cm). (B) SEM image of the aerogel of Figure A.

reduction of the PPO granules (whose diameter becomes roughly lower than  $1\ \mu\text{m}$ ). Thus, the maintenance of the fibrillar morphology of the s-PS in mixed gels and aerogels makes feasible PPO-rich monolithic aerogels.

The X-ray diffraction pattern of the mixed 90/10 PPO/s-PS aerogel (curve b) is compared in Figure 6 to the diffraction patterns of a pure s-PS aerogel (curve a) and a PPO powder (curve c).

The diffraction pattern of the pure s-PS aerogel (curve a) presents strong reflections at  $2\theta = 8.3, 13.5, 16.7, 20.5$  and  $23.3^\circ$  that are typical of the  $\delta$ -form.<sup>[11a]</sup> The diffraction pattern of the mixed 90/10 PPO/s-PS aerogel (curve b) clearly shows that a highly crystalline aerogel is obtained from the gel. The diffraction pattern of this mixed aerogel differs from the diffraction pattern of the pure PPO powder (curve c). In fact, for the pure PPO powder, diffraction peaks at  $4.95^\circ, 7.65^\circ, 12.3^\circ, 16.1^\circ$  and  $21.5^\circ$  are observed while the 90/10 PPO/s-PS aerogel

presents diffraction peaks at  $4.6, 7.3, 11.6, 14.9$  and  $21.4^\circ$ . This shift indicates a strong influence of s-PS on PPO crystallization.

Total surface area ( $S_{\text{BET}}$ ) and micropore area ( $S_{\text{micro}}$ ), for the mixed 90/10 PPO/s-PS, as obtained from  $\text{N}_2$  adsorption measurements are equal to  $483\ \text{m}^2/\text{g}$  and  $172\ \text{m}^2/\text{g}$ , respectively while for the pure s-PS aerogel the values of  $S_{\text{BET}}$  and  $S_{\text{micro}}$  are  $206\ \text{m}^2/\text{g}$  and  $27\ \text{m}^2/\text{g}$ , respectively. These data indicate that by using a blend of s-PS and PPO to prepare the native thermoreversible gel, it is possible to obtain monolithic aerogels characterized by a nanoporous crystalline phase and high surface areas.

### Nanoporous PPO Films

Semi-crystalline PPO films with nanoporous crystalline phases can be easily obtained by exposing amorphous PPO films to solvent vapours and then removing the solvent by treatment with supercritical carbon dioxide. The x-ray diffraction patterns of crystallized PPO films are similar to those of PPO semi-crystalline powders obtained from gels being reported in Figure 1.<sup>[16]</sup>

The propane sorption isotherms and diffusivity at  $30^\circ\text{C}$  in amorphous PPO and semi-crystalline PPO films obtained by benzene and  $\text{CCl}_4$  vapour treatments of amorphous films are reported in Figure 7A and 7B, respectively.

Figure 7A clearly shows that the propane solubility is lower for the amorphous PPO film as compared with semi-crystalline PPO films. This result which is clearly opposite to the behaviour commonly observed in semi-crystalline polymers, is due to the presence of nanoporous crystalline phases. It is worth noting that the same behaviour was also observed with other penetrants such as  $\text{CO}_2$ ,<sup>[16]</sup> methane,<sup>[16]</sup> and propene.<sup>[16]</sup>

We can observe in Figure 7B a significant increase of the propane diffusivity by moving from amorphous to semi-crystalline PPO. The larger diffusivities for semi-crystalline PPOs as compared to amorphous PPO appears quite unexpected as usually the presence of semi-crystalline

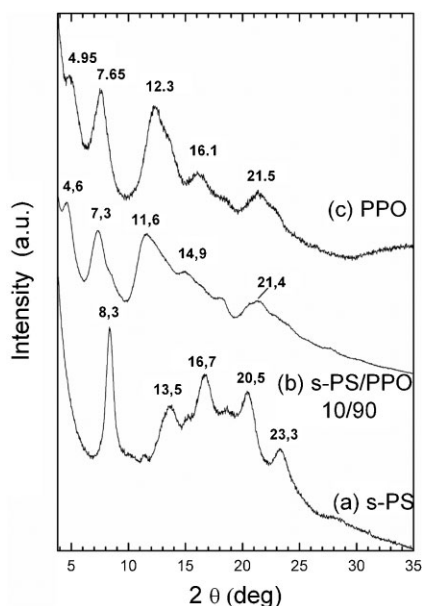


**Figure 6.**

X-ray diffraction patterns ( $\text{CuK}\alpha$  radiation) of PPO/s-PS gels in DCE, prepared with a polymer content of 20wt%, after complete solvent extraction by supercritical  $\text{CO}_2$ , for different PPO fractions: (a) s-PS aerogel; (b) s-PS/PPO (10/90) aerogel; (c) PPO powder.

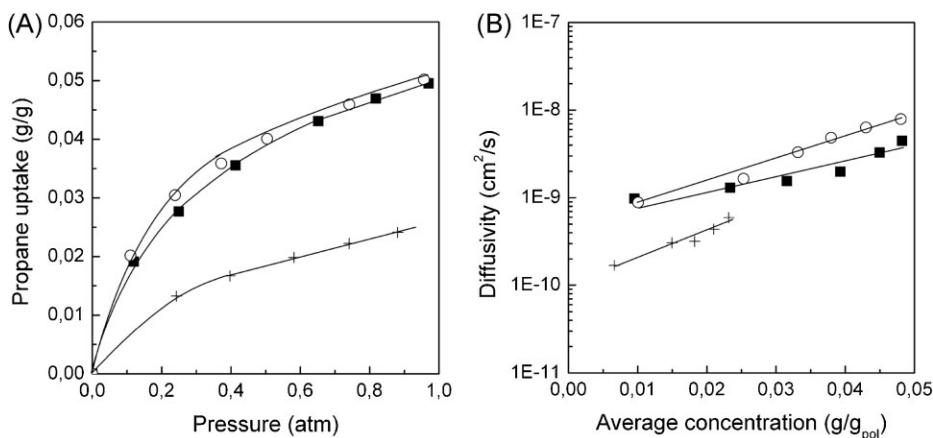


**Figure 7.**

Propane sorption isotherms (A) and diffusivity (B) at 30 °C in an amorphous PPO film (+), benzene-crystallized (■) and CCl<sub>4</sub>-crystallized (○) semi-crystalline films. (A): continuous lines are only guides for the eye. (B): continuous lines represent an exponential interpolation.

regions leads to an increase of the tortuosity of the penetrant molecular path thus reducing the diffusivity. This behavior can be again attributed to the nanoporous structure of the crystalline domains.

## Conclusion

In this paper it has been shown that extraction with supercritical carbon dioxide of the solvent of PPO gels obtained leads to powder samples with nanoporous crystalline phases. These materials which are characterized by high surface area values (up to 550 m<sup>2</sup>g<sup>-1</sup>) present a high benzene uptake from vapour phase already for low activity. The use of a small amount of s-PS allows the formation of a fibrillar 3D network in the mixed s-PS/PPO gels and nanoporous monolith aerogels can be easily obtained after solvent extraction. These nanoporous-crystalline PPO rich aerogels present high surface areas (up to 480 m<sup>2</sup>g<sup>-1</sup>) due to the presence of the crystalline cavities of PPO and good handling properties due to the s-PS fibrillar 3D network, and hence seems particularly suitable for removal of traces of organic pollutants from water and air.

Subatmospheric gas sorption experiments have shown that PPO crystalline films are characterized by larger gas sorption capacity and diffusivity as compared to the amorphous films. These peculiar mass transport properties which are due to the nanoporous nature of the crystalline phase make semi-crystalline PPO films potentially interesting for membrane based gas separation processes.

**Acknowledgements:** Financial support of the “Ministero dell’Istruzione, dell’Università e della Ricerca” (Prin 2010-2011) is gratefully acknowledged. The authors are indebted to Dr. Jenny Vitillo of University of Turin for the N<sub>2</sub> adsorption measurements and to Dr. Stefano Cardea of the Università degli Studi di Salerno for SEM images.

- [1] J. M. Guenet, in “*Polymer-solvent molecular compounds*”, Elsevier Ltd., Oxford **2008**.
- [2] (a) E. D. T. Atkins, D. H. Isaac, A. Keller, K. J. Miyasaka, *Polym. Sci., Polym. Phys. Ed.* **1977**, 15, 211. (b) J. M. Guenet, G. B. McKenna, *Macromolecules* **1988**, 21, 1752. (c) S. El Hasri, B. Ray, A. Thierry, J. M. Guenet, *Macromolecules* **2004**, 37, 4124.
- [3] G. Guerra, C. Daniel, P. Rizzo, O. Tarallo, *J. Polym. Sci. Polym. Phys. Ed.*, **2012**, 50, 305 and references 24–40 herein.

- [4] (a) M. Iuliano, G. Guerra, V. Petraccone, P. Corradini, C. Pellecchia, *New Polym. Mater.* **1992**, 3, 133. (b) C. De Rosa, V. Petraccone, G. Guerra, C. Manfredi, *Polymer* **1996**, 37, 5247. (c) O. Tarallo, G. Esposito, U. Passarelli, V. Petraccone, *Macromolecules* **2007**, 40, 5471. (d) G. Esposito, O. Tarallo, V. Petraccone, *Eur. Polym. J.* **2007**, 43, 1278.
- [5] V. Petraccone, O. Tarallo, V. Califano, V. *Macromolecules* **2003**, 36, 685.
- [6] (a) M. Yokoyama, H. Ishihara, R. Iwamoto, H. Tadokoro, *Macromolecules* **1969**, 2, 184. (b) J. J. Point, C. Coutelier, *J. Polym. Sci., Polym. Phys. Ed.* **1985**, 23, 231. (c) L. A. Belfiore, E. Ueda, *Polymer* **1992**, 33, 3833. (d) L. Paternostre, P. Damman, M. Dosiere, *Macromolecules* **1999**, 32, 153.
- [7] (a) A. K. Dikshit, A. K. Nandi, *Macromolecules* **2000**, 33, 2616. (b) D. Dasgupta, S. Malik, A. Thierry, J. M. Guenet, A. K. Nandi, *Macromolecules* **2006**, 39, 6110.
- [8] (a) H. Kusuyama, M. Yakase, Y. Higashihata, H. T. Tseng, Y. Chatani, H. Tadokoro, *Polymer* **1982**, 23, 1256. (b) A. Saiani, J. Spevacek, J. M. Guenet, *Macromolecules* **1998**, 31, 703. (c) A. Saiani, J. M. Guenet, *Macromolecules* **1999**, 32, 657.
- [9] C. Daniel, J. G. Vitillo, G. Fasano, G. Guerra, *ACS Appl. Mater. Interfaces* **2011**, 3, 969.
- [10] (a) A. Factor, G. E. Heinsohn, L. H. Vogt, Jr., *Polym. Lett.* **1969**, 7, 205. (b) M. Barrales-Rienda, J. M. G. Fatou, *Kolloid Z. u. Z. Polym.* **1971**, 244, 317. (c) S. Horikiri, *J. Polym. Sci. A2* **1972**, 10, 1167. (d) J. Hurek, E. Turska, *Acta Polimerica* **1984**, 35, 201. (e) O. Tarallo, V. Petraccone, C. Daniel, G. Fasano, P. Rizzo, G. Guerra, *J. Mater. Chem.* **2012**, 22, 11672.
- [11] (a) C. De Rosa, G. Guerra, V. Petraccone, B. Pirozzi, *Macromolecules* **1997**, 30, 4147. (b) G. Milano, V. Venditto, G. Guerra, L. Cavallo, P. Ciambelli, D. Sannino, *Chem. Mater.* **2001**, 13, 1506.
- [12] V. Petraccone, O. Ruiz de Ballesteros, O. Tarallo, P. Rizzo, G. Guerra, *Chem. Mater.* **2008**, 20, 3663.
- [13] (a) C. Manfredi, M. A. Del Nobile, G. Mensitieri, G. Guerra, M. Rapacciuolo, *J. Polym. Sci., Polym. Phys. Ed.* **1997**, 35, 133. (b) P. Musto, G. Mensitieri, S. Cotugno, G. Guerra, V. Venditto, *Macromolecules* **2002**, 35, 2296. (c) V. Venditto, A. De Girolamo Del Mauro, G. Mensitieri, G. Milano, P. Musto, P. Rizzo, G. Guerra, *Chem. Mater.* **2006**, 18, 2205.
- [14] P. Pilla, A. Cusano, A. Cutolo, M. Giordano, G. Mensitieri, P. Rizzo, L. Sanguigno, V. Venditto, G. Guerra, *Sensors* **2009**, 9, 9816.
- [15] C. Daniel, S. Longo, G. Fasano, J. Vitillo, G. Guerra, *Chem. Mater.* **2011**, 23, 3195.
- [16] M. Galizia, C. Daniel, G. Fasano, G. Guerra, G. Mensitieri, *Macromolecules* **2012**, 45, 3604.
- [17] C. Daniel, D. Zohvner, G. Guerra, *Macromolecules* **2013**, 46, 449.
- [18] (a) E. B. Gowd, N. Shibayama, K. Tashiro, *Macromolecules* **2007**, 40, 6291. (b) P. Rizzo, C. D'Aniello, A. De Girolamo Del Mauro, G. Guerra, *Macromolecules* **2007**, 40, 9470.
- [19] (a) C. Daniel, D. Alfano, V. Venditto, S. Cardea, E. Reverchon, D. Larobina, G. Mensitieri, G. Guerra, *Adv. Mater.* **2005**, 17, 1515. (b) C. Daniel, D. Sannino, G. Guerra, *Chem. Mater.* **2008**, 20, 577.
- [20] S. Figueroa-Gerstenmaier, C. Daniel, G. Milano, J. G. Vitillo, O. Zavorotynska, G. Spoto, G. Guerra, *Macromolecules* **2010**, 43, 8594.
- [21] C. Daniel, S. Longo, S. Cardea, J. G. Vitillo, G. Guerra, *RSC Adv.* **2012**, 2, 12011.